PCCP

ROYAL SOCIETY OF CHEMISTRY

PAPER

View Article Online
View Journal

Cite this: DOI: 10.1039/d6cp00680a

Monitoring the effects of salt background, alkalinity and temperature on MS2 bacteriophage behaviour *via* solvatochromism, metachromasia and chemical kinetics

Anna Laguta [ab]

Received 24th February 2026,
Accepted 23rd May 2026

DOI: 10.1039/d6cp00680a

rsc.li/pccp

Although this work deals with well-established methods and a well-known model system, it demonstrates innovative findings. These groundbreaking findings will be of interest to chemists, biologists, and medical professionals alike. This investigation is pure and provides a dataset for gaining an in-depth understanding of the interactions of the MS2 bacteriophage with inorganic and organic ions. The nanoparticle surface can be viewed as an unstructured continuum characterized by a zeta potential that governs interspecies interactions and depends on the ionic composition of the aqueous medium. Interactions with inorganic and organic ions should involve considering the surface as a discontinuum. Recently, empirical evidence has led to a patch-like model of the surface of MS2 with discrete positive and negative values of surface charge density. This work involves concepts of the solvatochromism of malachite green as a polarity-dependent factor, the metachromasia of crystal violet as an association-dependent factor, and the chemical kinetics of alkaline fading of these dyes to investigate interparticle interactions and ion exchange. Such combined techniques provide broadly applicable data for studying bacterial interactions with various charged species or other biological interfaces.

1. Introduction

The interaction of a viral particle with a receptor that it uses to target bacterial cells defines the first stage in infection by a bacteriophage.[1,2] The investigation of interparticle interactions provides a source of information for medical and biotechnological phage applications and for understanding the molecular interactions between the phage and host during the infection cycle and phage ecology.[3,4] Understanding the surface forces involved and the factors affecting interactions with individual molecules and ions is a way to investigate phage–host interactions. The majority of the physical properties of protein assemblies are due to charges and the ability of proteins to bind water (to be solvated).[5]

Bacteriophage MS2 resembles many human enteric viruses in terms of size and structural properties; according to Feng *et al.*,[6] MS2 could simulate virus behaviour better than Qβ in extreme acidic or alkaline solutions or at temperatures above 25 °C. Icosahedral bacteriophage MS2, which infects Gram-negative bacteria (*Escherichia coli*), consists of a protein capsid and an enclosed RNA genome.[7,8] A recently constructed full-atom model of the protein layer demonstrated a 28 nm protein capsid with a thickness of 2.5 nm and pores of 1.1 nm.[8,9] In earlier studies, the structure of the MS2 capsid was determined by X-ray diffraction.[10] In contrast to the commonly accepted hypothesis that the virus is hydrophobic, the MS2 surface appears to be hydrophilic in solution.[11] The bacteriophage has a negative zeta potential in the physiological pH range and is stable in the pH range of 3–11.[6] Infectivity, enumerated by the plaque assay method using the double-agar-layer technique according to ISO 10705-1, alters: it is $-1\log_{10}$ at 60 °C and $-8\log_{10}$ at 72 °C.[12]

The surface layer of protein particles is a double electric layer that is typically characterized by negative electrophoretic mobility at physiological pH.[13] Attraction energy dominates between anionic hydrophobic particles at very short ($\rightarrow 0$) and long ($\sim 10^2$ nm) distances, while repulsion energy dominates at intermediate distances.[14,15] A hydrophilic surface should provide a pronounced solvation shell. A decrease in zeta potential promotes flocculation at high ion concentrations.[11,16] For example, the influence of Na^+ on reducing hydration repulsion forces and the local water structure promotes membrane fusion of *E. coli* and the local aggregation of the bacterial potassium channel KcsA.[17] Punch *et al.* showed that infection by an enveloped bunyavirus depends on the local ionic composition: locally high K^+ concentrations enhance viral spike–membrane interactions.[18]

[a] *University of Chemistry and Technology Prague, Technická 5, 166 28 Prague 6, Czech Republic*
[b] *V. N. Karazin Kharkiv National University, Svoboda Square 4, Kharkiv 61022, Ukraine. E-mail: laguta@karazin.ua*

Focusing on classical theories and direct typical methods of analysing biological objects can omit important details and peculiarities. In recent studies, the application of spectrophotometric method for the determination of pK_a indicators bound by the MS2 surface[11] and MD computer simulation data[9,11] revealed the twofold surface effects and the mosaic-patchy surface character. Nevertheless, locally, the surface can be fitted within a double-layer framework.

Herein, solvatochromism, metachromasia, and chemical kinetics approaches are used.[19,20] The dependence of the reaction rate on reagent concentration provides insight into interparticle interactions, surface acidity, and ion exchange at the interface, as determined from the reaction between hydroxide ion and a probe that has a strong affinity for the phage surface.[21] In recent work,[11] it has been shown that anionic probes have weak affinity for MS2, and cationic probes, upon binding, are located in the negative domain of the capsid mosaic structure. Cationic triphenylmethane dyes – crystal violet (CV) and malachite green (MG) – were chosen as probes for the investigation; thus, the observed features primarily characterize the negative domain of the phage mosaic structure in aqueous and alkaline media. The lipophilicity of CV^+ (chloride) and MG^+ (chloride) is characterised by $\log P_{ow}$ values of 0.51 and 0.62.[22] The effect of CV on bacteriophages is of long-standing interest.[23] CV suppressed the intracellular multiplication of the lactic Streptococcus bacteriophage which permitted growth of the host cells.[24] Unlike methylene blue, CV did not inhibit the Staphylococcus bacteriophage.[25] The photobiocidal performance of visible-light-activated cationic triphenylmethane dyes against MS2 bacteriophages was reported by Shin *et al.*[26]

Classical ideas (ref. 27 and 28) about the shoulder band in the visible region of the spectrum of CV are based on two types of absorption bands for a planar molecule, as absorption is polarized along the mutually perpendicular x and y directions in the molecule.[2] Depending on the type of solvent, conditions, and symmetry of the dye, a shoulder absorption band can coincide or split into two bands.[29] Contemporary interpretations present a propeller structure (D_3 symmetry) for the ground state and a pyramidal structure (C_3 symmetry) in which three bonds of the central atom are bent. Ref. 30 demonstrates that phenyl torsion makes the CV spectrum sensitive to environmental perturbations. A recent study[31] presented twelve strong correlations for MG between the torsion and valence angles in various combinations, forming two absorption peaks with spacing between them. This paper revealed that CV^+ binding to a phage pronouncedly affects the equilibrium of the isomers, while MG^+ does not. Overall, the work provides a set of empirical facts and approaches for studying various biological nanotypes.

2. Materials and methods

Crystal violet (CV, Acros Organic) and malachite green (MG, Thermo Scientific) were of high-purity grade. Sodium chloride, calcium chloride, rubidium chloride (99.5% purity, AnalaR), potassium chloride, sodium iodite, sodium acetate, sodium salicylate, sodium glycolate (NaGly, 97% purity, Alfa Aesar), sodium nitrate (99% purity, Fluka), and sodium butyrate (98% purity, Alfa Aesar) were obtained from the sources shown.

All solutions were prepared using distilled water (pH = 5.8). A stock solution of NaOH was prepared from a saturated solution and kept protected from the atmosphere. Working solutions (10 mL) were prepared by the volumetric method.

The bacteriophage MS2 (ATCC 15597-B1) and its host *Escherichia coli* (*E. coli*) strain C-3000 (ATCC 15597) were obtained from American Type Culture Collection (ATCC). *E. coli* bacteria were cultured in Lennox L Broth medium (Melford Laboratories) at 37 °C and infected with the MS2 phage at the middle log-phase. The lysate was centrifuged using Amicon Ultra-175 (Ultracel-100 K, regenerated cellulose, 10 000 MWCO) at 10 000g for 15 min (7810R Eppendorf centrifuge) to remove cell debris after the complete lysis of the bacteria, and then centrifuged again at 100 000g for 4 h (thin-wall polypropylene tubes, 14 × 89 mm) to pellet the phage particles at 4 °C. MS2 was resuspended in the buffer system (pH = 7.5; 5 mM (1 M = 1 mol L^{-1}) TRIS, 150 mM NaCl, 5 mM $CaCl_2$, and 5 mM $MgCl_2$; the ionic strength is 0.18 M). The created suspensions of MS2 phages were kept at 4 °C before use. The plaque assay method was used to enumerate MS2 phages. 10-fold serial dilutions in LB medium of MS2 stock solutions were inoculated onto a double-agar layer. Infective MS2 phage concentrations were defined as the number of plaque-forming units per mL (PFU per mL). The final concentration of purified phages was 10^{18} PFU per mL. The MS2 amount in the working solution was 4×10^{15} PFU per mL. The working solution was examined immediately after the addition of an aliquot of the prepared phage solution, and the concentrations of buffer components in the working solution were negligible; the pH and ionic composition of the working solution were controlled by aliquots of alkali and/or salt. Negligible effects from the absorption and scattering of the colloidal system on the analysis of the dye's visible absorption spectra were ensured by using low working MS2 concentrations. Its absorption band rises in the UV region.

Absorbance was measured on a Thermo Scientific Multiskan GO Microplate spectrophotometer at 25 °C. CV^+ and MG^+ cations, which have a high extinction coefficient in the vis-band of absorption spectra, form colourless carbinol in the nucleophilic addition reaction of the hydroxide: $Dye^+ + HO^- \rightarrow (Dye)OH$. In alkaline media, dye fading proceeds irreversibly. The rate constant was determined spectrophotometrically at a temperature of 25 °C by measuring the absorbance at λ_{max} within 30 min to 2 h. The rate constant of a bimolecular reaction under pseudo-first order conditions of $c_{HO^-}/c_{Dye} > 100$ can be easily determined. The reaction is of 1st order with respect to the dye, therefore:

$$v = -dc_{Dye}/dt = k' c_{Dye} \quad (1)$$

$$k' = k c_{HO^-} = \text{const} \quad (2)$$

$$k' = \left(\frac{1}{t}\right) \ln\left(\frac{c_{Dye,0}}{c_{Dye,t}}\right), \quad (3)$$

$$\ln A_t = \ln A_0 - k' t \quad (4)$$

where k is the rate constant of the second-order reaction; c_i is the concentration of 'i'; the subscripts '0' and 't' correspond to the values at the initial time and time t; k' is the rate constant of the pseudo-first order reaction; and A is the absorbance. The standard error of the determination of k' values was less than 5%. The higher rate constant for MG^+ limits the determination of k' and the maximum dye absorption under highly alkaline conditions using this method.

3. Discussion

3.1. A spectral approach to the study

Recent works[11,16] that regard the outer surface of the MS2 capsid as a discontinuum containing certain charged groups emphasize a 'mosaic-patches' model of the charge distribution, which forms discrete positive and negative domains, in contrast to the negative electrophoretic mobility that characterizes the surface as a whole unstructured continuum. At pH values of 7–11, the negative charges are provided by the carboxylate of side chains as Brønsted bases with pK_a = 3.7 and 4.2 (ref. 32) for aspartic and glutamic acids (see Fig. 1 and Table S1); also worth keeping in mind are phenolic hydroxyl with pK_a = 9.8–10.4 (ref. 5) for tyrosine, and the cysteine sulfhydryl group with pK_a = 8–8.5 (ref. 5). Charges in the guanidino group (pK_a = 11.6–12.6 (ref. 5) and 13.8 (ref. 33)) and the lysine side chain (pK_a = 10.5 (ref. 34)) create positive charges at neutral pH. The distribution of counter ions from the MD computer simulation data shows a lower Na^+ concentration at the outer surface (*i.e.*, a diffuse layer of cations) than that of Cl^- ions at the inner surface (*i.e.*, a dense layer of anions).[9] In general, ionic dyes bind predominantly by electrostatic attraction,[11] thus the charged domain can be viewed as an active site on the phage surface for dye binding.

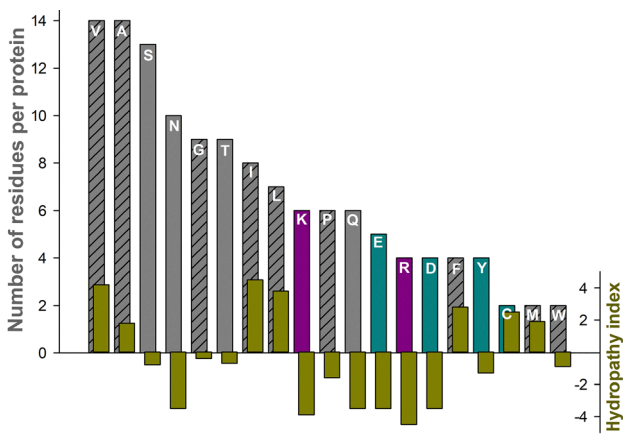

Fig. 1 Some characterization data for the 129 protein residues of the MS2 capsid: V, valine; A, alanine; S, serine; N, asparagine; G, glycine; T, threonine; I, isoleucine; L, leucine; K, lysine; P, proline; Q, glutamine; E, glutamate; R, arginine; D, aspartate; F, phenylalanine; Y, tyrosine; C, cysteine; M, methionine; and W, tryptophan. Examples with side-chain groups with pH-dependent charge are highlighted in dark cyan (0/−) and dark pink (+/0), while nonpolar groups have a hatched pattern.[39–41]

The mentioned pK_a values should be considered, taking into account that surface effects may correct these values.[35] For example, *p*-nitrophenol (charge type of acid–base couple: 0/−) and neutral red (+/0) exhibited ΔpK_a values of −0.36 and +1.01 on positive and negative MS2 domains, respectively.[11] Moreover, the tight packing of carboxyl may be accompanied by the formation of hydrogen bonds with neighboring COOH groups. A prime example is micelles of cholic acid, which are characterized by a pK_a value of 5.2, compared to pK_a = 4.98 for the monomer,[36,37] whereas in a binary mixed micelle, there are no bonds between the anions of deoxycholic acid.[38]

Some dyes – β-dinitrophenol (0/−), γ-dinitrophenol (0/−), *p*-nitrophenol (0/−), neutral red (+/0), hexamethoxy red (+/0), and rhodamine B (+/0) – did not change the wavelength of the absorption maximum, λ_{max}, when bound to the MS2 surface, which is intrinsic to well hydrated surfaces.[11,16] Binding of the indicators quinaldine red (2+/+), standard Reichardt's dye (+/±), bromothymol blue (−/2−), ethyl ester of fluorescein (0/−), β-dinitro-4-*n*-decylphenol (0/−), and *n*-decyl ester of fluorescein (0/−) was not significant in the context of studying their acid–base properties at 1×10^{-5} M dye and 5×10^{11} PFU per mL capsid MS2.[11] With these examples in mind, phage–dye interactions were studied using cationic triphenylmethane probes that exhibit solvatochromism and metachromasia. Solvatochromism of MG^+ results in λ_{max} of 614 (and 426) nm in water,[42] 620 nm in methanol and acetone,[43] and 621 nm in ethanol.[44] CV predominantly exists as an ion-pair in non-polar organic solvents (λ_{max} = 531 nm and 537 nm in cyclohexane and toluene, respectively); the cation has λ_{max} = 586 nm in methanol; 590 nm in water; and 595 nm in glycerol.[45]

In the MS2 solution, the binding of MG is accompanied by a pH-dependent bathochromic shift (Fig. S1):

c_{NaOH}, mM	0.2	0.4	0.6	0.9	1.3	1.8	2.7	3.5	4.4
λ_{max} (MG), nm	619	619	619	619	620	619	620	621	621
	426	426	426	427	426	428	428	427	427

For comparison, λ_{max} of MG was 619 nm in cationic micelles of CTAB, 624 nm in nonionic ones of Brij-35, 625 nm in zwitterionic ones of DMDAPS, and 626 nm in anionic ones of SDS.[46] The stronger shift in micellar systems aligns with expectations: (i) the probe is able to penetrate deeper between the surfactant head-groups, (ii) micelles have a decreasing polarity gradient toward the core,[11,47] and (iii) there is weaker hydrophobicity/more sufficient hydration of the cationic dye localization site on the MS2 phage. The domain for cationic dyes represents a patch with a negative charge density in terms of the mosaic MS2 surface. The anionic surface groups provide surface hydration by forming hydrogen bonds with water molecules. The bathochromic shift may be attributed to a decrease in the polarity domain. According to the pK_a values of arginine and lysine side chains, in alkaline solutions at a pH of 10.5, half of the positive lysine groups are deprotonated, and

for guanidine, this value is higher. Also, at this pH, phenolic hydroxides exist mainly in their deprotonated form. This generally reduces the surface density of positive charges and slightly increases the surface density for negative charges compared to that at neutral pH.

Switching off the positive surface charges was revealed experimentally by considering the surface as a continuum. These deprotonation effects lead to the following zeta potential values of MS2 (measured by electrophoretic mobility[11] on a Zetasizer Nano ZS Malvern Instrument): −37, −39, −47, and −42 mV in the absence of NaOH and with 0.1, 1, and 5 mM NaOH, respectively, whereas no effect on colloid stability was detected from size measurements. Some protein dehydration is expected due to the difference in hydration states between the protonated and deprotonated forms.[48] This affects on hydrophilization and is observed as a bathochromic shift of the dye.

The next subtle alkali effect is related to the alteration of the association of the surface groups with CV^+. The pronounced ability of CV to undergo metachromasia helps to verify this empirically.[49] The spectrum of CV in the MS2 solution is characterized by a broad band with two maxima of equal observed intensity at 544 and 588 nm (Fig. 2). As such, metachromasia for CV^+ was detected in a wider range of systems compared to MG^+, which contains one fewer amino group. Methyl violet typically behaves similarly to CV. This phenomenon originates from various phenomena caused by different conditions, including aggregation, association, and the influence of the solvent (see also the Introduction).[50] Therefore, in biological systems, each case must be carefully analyzed. Regarding the solvent polarity effect, based on the literature λ_{max} values cited above, metachromasia is expected when polarity decreases significantly. Aggregation implies the interaction of several dye molecules on the surface, which in phage-free water appears at $c_{CV} \sim 10^{-3}$ M and is characterized by λ_{max} = 550 nm (dimer) or 520 nm (trimer).[51] In a solution of CV and sodium dodecylsulfate of equal concentrations of 10^{-5} M, premicellar aggregates of CV^+DS^- ion pairs appear as a short-frequency peak due to the interactions of dye chromophores with each other, but in SDS micelles, CV^+ (species isolated from each other) exhibits a solvatochromic shift without metachromasia.[52] Association implies interaction between dye cations and surface anions. The formation of ion pairs with perchlorate and no association with chloride ions in the aqueous phase is known.[53] The existence of an association with chloride was observed in micelles of cetyltrimethylammonium chloride.[54] The formation of CV^+Cl^- is typical of solvents with a low dielectric constant.[55] Herein, increasing the dye concentration (Fig. S1) in MS2 solution without added alkali did not result in a rise in the short-wavelength peak; the reasoning for this is based on the predominance of an ion pair formed with the outer surface anions, and this does not confirm the possibility of dye aggregation. This association can be hypothesized in terms of supramolecular salt bridges[56] between the carboxyl groups of glutamate/aspartate side chains and CV^+. Regarding the anionic groups of RNA, there is no reliable information in the literature known to us about the effect of CV on RNA uncoating. RNA interacts with all 90 dimers of the shell protein and is located directly beneath the protein capsid.[57] RNA forms a branched network of stem-loops that are almost all located in one half of the capsid.[58] Three bands of RNA density in the radial density distribution are located 3 nm and 7 nm under the capsid and in the centre of the capsid, respectively.[59] The diameter of 30 pores is about 1.1 nm in the capsid wall, allowing water, Na^+ and Cl^- ion transport.[8] CV is 0.44 nm in width and 1.3 nm in length.[60] It is not excluded that the dye may interact with RNA, and this hypothesis has already been proposed in ref. 61. For example, metachromasia of CV was observed for other species with ionized phosphate groups.[62,63] It is worth noting here a fact obtained during the temperature investigation (presented below): at temperatures above the phage destruction temperature, the RNA adsorption peak remained, but metachromasia did not. Therefore, the arguments are based on the interaction of the virion as a whole with the dye, rather than on specific interactions between RNA and the dye.

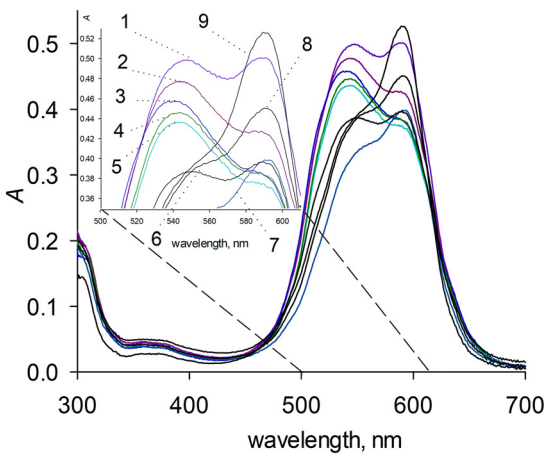

Fig. 2 Absorption spectra of 1×10^{-5} M CV in solutions of 4×10^{15} PFU per mL MS2 at 25 °C at different c_{NaOH} values (mM): without added alkali (1); 0.4 (2); 1 (3); 3 (4); 5.5 (5); 6.5 (6); 7.5 (7); 8.8 (8); and 10 (9).

Furthermore, the dye's spectrum in protein dimers did not appear unusual. Protein dimers was obtained by (i) the 1 : 3 dilution of MS2 phage in cold glacial acetic acid, (ii) incubation for two hours at 4 °C, and centrifugation at 12 000*g* for 10 minutes at 4 °C to pelletize precipitated RNA and maturase, (iii) dialyzing against 10 mM acetic acid with 50 mM NaCl using regenerated cellulose tubing (15 kDa MWCO); and (iv) assaying for the amount of protein stained with Brilliant Blue *via* agarose gel electrophoresis.

Back to the effects of alkali, a strong predominant short-wavelength peak at 537 nm was observed in MS2 systems with c_{NaOH} of 2–4 mM (Fig. S1b). At c_{NaOH} ~7 mM (Fig. 2 at 1×10^{-5} M CV and Fig. S1 at 1×10^{-4} M CV), the peaks are again level in intensity. It is noteworthy that these alkali concentrations create pH around to the pK_a of cationic groups of the phage. At $c_{NaOH} \sim 7$ mM, they have already dissociated significantly (at this pH, only half of the guanidine remains protonated). Further addition of alkali again changes the spectrum and results in a single peak at 590 nm. It appears that the

deprotonation of groups destabilizes MS2. According to the inactivation rates obtained by Feng *et al.*,[6] when the initial concentration was 4×10^{15} PFU per mL, concentrations of 3.8×10^{15} and 2.3×10^{15} PFU per mL remained after 1 h at pH 10 and 11, respectively, at 25 °C.

This hypothesized association is thought to be dependent on inert salt. Empirical evidence is in agreement with this hypothesis and indicates that cations have different abilities to screen surface anions (Fig. 3 and Fig. S2–S17). Absorption spectra were obtained in the presence of salt without alkali and in alkaline media. The absorption spectra of MG are unremarkable and show (in general) reduced bathochromic shifts in the presence of salts (Table S2), *i.e.*, the dye remains in the bound state. The kinetics approach discussed below also demonstrates this binding. The CV absorption spectra are more revealing and demonstrate a decrease in the degree of association with salt addition, except for 1 mM sodium iodide, butyrate and salicylate; this continues the trend identified above when considering the influence of the alkali cation on the zeta potential. The zeta potential decreases, and the values are −35, −34, −9, −7, and −6 mV at 0, 30, 60, 100, and 800 mM NaCl, respectively, and −33, −25, −19, −12, and −11 mV at 0.1, 0.5, 1, 5, and 10 mM $CaCl_2$, respectively.[16] A comparison of the effects of cations with a given anion (Fig. 3 and Fig. S2–S9) showed an enhanced affinity for the surface in the order: Na^+ (−365 kJ mol^{-1}[64]) < K^+ (−295 kJ mol^{-1}[64]) < Rb^+ (−275 kJ mol^{-1}[64]) < Ca^{2+} (−1505 kJ mol^{-1}[64]), which is consistent with the notion that weakly hydrated ions have a high affinity for the surface (hydration energies in parentheses) and that there are enhanced electrostatic forces with increasing cation charge. The anion effect at the given cation (Fig. 3d) was dominant only at the lowest salt concentration (*i.e.*, when the cation had a weak effect) and had a smaller influence on the association than the HO^- effect discussed above. Weakly hydrated But^-, Sal^- (−282 kJ mol^{-1}[64]), and I^- (−275 kJ mol^{-1}[64]) enhanced the short-wavelength CV^+ band compared to Cl^- (−340 kJ mol^{-1}[64]) and NO_3^- (−300 kJ mol^{-1}[64]). In previous work,[11] dinitrophenols were bound by MS2; accordingly, salicylate should also bind to MS2. Note that in the presence of Ca^{2+}, association is not observed in the spectra, despite the fact that dynamic light scattering detected phage nanoparticles in these systems and λ_{max} (CV) = 591 nm. At 0.05 M, all studied salts prevent the electrostatic interaction of the dye with surface groups. Sodium hydroxide in a mixture with alkali metal salt enhances the short-wavelength peak only at the lowest salt content (Fig. S2–S17). The effects of anions are more clearly demonstrated by chemical kinetics (see below).

Moving on, the effect of temperature on the absorption spectrum of CV^+ in a solution containing 4×10^{15} PFU per mL MS2 was investigated. UV and visible absorption spectra of CV in phage solutions without and with electrolyte were obtained by the stepwise gentle heating of the solution (Fig. 4 and Fig. S18). A set of spectra shows that above 65 °C (without salt addition), the short wavelength peak of CV decreased in intensity. The absorption spectrum at 95 °C has a maximum at 592 nm. When the solution was cooled, the short-wavelength dye peak did not appear, indicating that in the phage-free solution, the dye exists as non-associated monomers (see the discussion above regarding RNA). This finding may serve as evidence that dye metachromasia is caused by interaction with the intact virus structure.

According to Brié *et al.*,[12] the MS2 phage remains unchanged in capsid aspect, genome, size, and electrophoretic mobility up to 60 °C, while 10 min of heating at 72 °C results in a decrease in population and a 1.68-fold increase in size. The critical disruption temperature of the MS2 phage was noted as being above 60 °C (around 66–67 °C), which is consistent with the tipping point temperature observed here. As the temperature is as expected, the dye at this concentration does not affect phage stability. No significant changes in the persistence of the genome were observed by RT-PCR at temperatures of 60 and 72 °C.[12] Note that when heated at 75 °C for 20 min, the Salmonella typhimuriam bacteriophage P22 forms a wiffle-ball structure with 10 nm pores caused by the release of pentons that are normally present at each of the 12 icosahedral fivefold positions.[65] When exposed to a temperature higher than the critical temperature (72 °C), the particles were disrupted and the genome became available for RNases.[12]

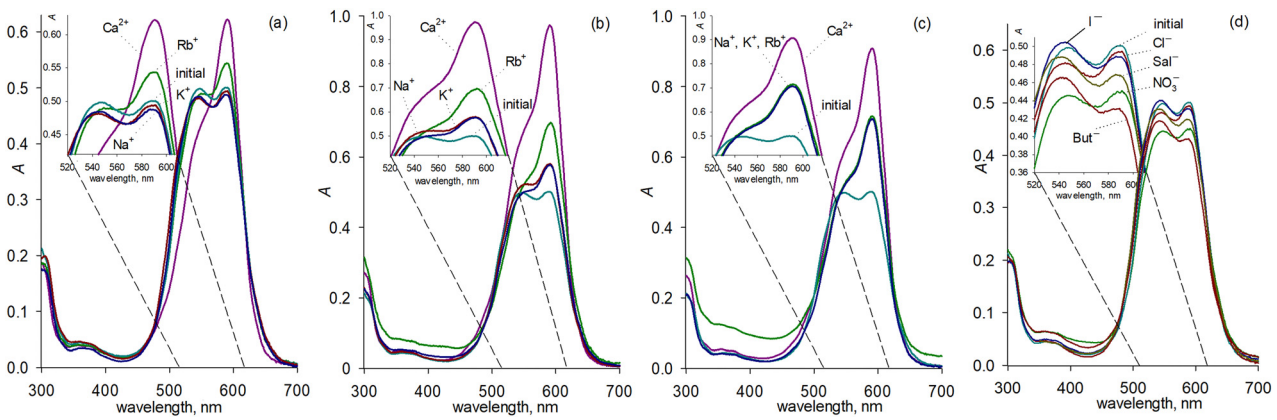

Fig. 3 Absorption spectra of 1×10^{-5} M CV in solutions of 4×10^{15} PFU per mL MS2 and salts: chloride salts of Ca^{2+}, Rb^+, K^+, and Na^+ at 1 mM (a); 10 mM (b); and 50 mM (c); and 1 mM NaCl, NaI, NaSal, NaBut, and $NaNO_3$ (d).

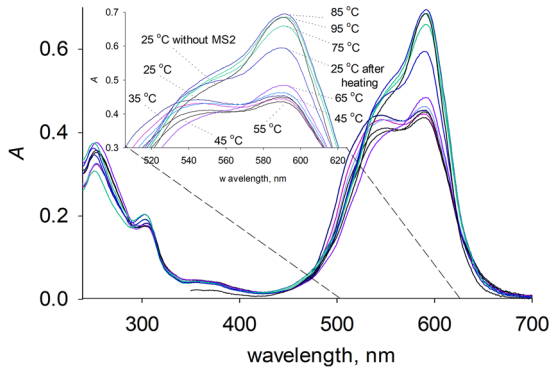

Fig. 4 Influence of temperature on absorption spectra of CV^+ in a solution of 4×10^{15} PFU per mL MS2.

The salt effect (Fig. S18) results in a tipping point temperature of 55 °C (with 10 mM NaCl). The dye maximum after heating is at 591 nm (at 0.01 M NaCl).

3.2. Chemical kinetics investigation

The main part of the experiments corresponds to a pH less than the pK_a value of the guanidinium group. The observed reaction rate under the condition of the partial binding of reagents is a function of their concentration:

$$k_{obs}[Dye_{total}][HO_{total}^-] = k'_{obs}[Dye_{total}] = k_w[Dye_w][HO_w^-] + k_b[Dye_b][HO_b^-],$$

where the subscripts obs, total, b, and w indicate the observed value, total value, bound value, and unbound value, respectively.

The concentration of bound hydroxide ions on the surface where dye is located is a function of both surface potential (eqn (5)) and counterion concentration, $[X^-]$, (eqn (6)) as follows:

$$P_{HO^-} = \exp(F\Psi/RT), \quad (5)$$

where P_{HO^-} is the distribution coefficient of hydroxide ions; Ψ is the electrostatic potential of the surface where the dye is located; F is the Faraday constant; R is the gas constant; and T is the absolute temperature; and:

$$HO_s^- + X_w^- \underset{}{\overset{K_{X^-}^{HO^-} = \frac{[HO^-]_w[X^-]_s}{[HO^-]_s[X^-]_w}}{\rightleftharpoons}} HO_w^- + X_s^- \quad (6)$$

These statements acquired from micellar rate effects are useful for the investigation of the capsid interaction with ions, as well as reactant interactions on the phage surface.[66] In solution with c_{NaOH} = 0.2 mM, at which the association of CV with surface groups is observed (Fig. 2), the second-order rate constants for $CV^+ + HO^-$ and $MG^+ + HO^-$ reactions are 0.025 M^{-1} s^{-1} and 0.87 M^{-1} s^{-1}, compared to 0.21 M^{-1} s^{-1} and 1.79 M^{-1} s^{-1} in aqueous solution at 25 °C and with I = 0.2 mM. The observed rate constant at the interface is determined by several variables such as the polarity and ionic strength of the microenvironment (the difference in k_w and k_b), as well as surface charge (mainly the effect on P_{OH^-}).[21,52,66] For example, when binding the dyes, anionic micelles of sodium dodecylsulfate strongly decelerate these reactions mainly in view of the repulsion of hydroxide ions; cationic micelles strongly accelerate them due to the attraction of hydroxide ions; and nonionic and zwitterionic micelles weakly accelerate them on account of a decrease in the polarity of the microenvironment, enhancing interactions between cations and anions (the polarity effect).[19]

Paralleling surfactant micelles, the observed influence of the MS2 phage corresponds to the following: (i) the dyes localize to the negative groups; and (ii) the observed rate constant becomes smaller than that corresponding to the bulk concentration of alkali. Consequently, HO^- anions are present in the negatively charged domain in lower concentrations than in the bulk phase. From the observed deceleration, the microenvironment in the domain cannot be considered low-polarity either, since a significant decrease in polarity compared to the bulk phase should accelerate the reaction.[67] This effect is definitely not a major one, which is in agreement with Vodolazkaya *et al.*[11] and contradicts the generally accepted hypothesis that this viral particles are hydrophobic. At the same time, some acceleration was observed with the initial increase in alkali concentration from 0.4 mM to 4 mM (Fig. 5), which corresponds to the dissociation of the phage's cationic groups. In general, the acceleration is small and can be attributed to an increase in HO^- concentration and the effect of reduced hydrophilicity. The prerequisite for this reduction is some surface dehydration predicted from the enhanced solvatochromism of MG and metachromasia of CV (when the alkali concentration increases to the inflection point of the kinetic curve shown in Fig. 5). The further rapid growth depends on a rise in c_{alkali}, at which point the CV spectrum forms a long-wave peak, *i.e.*, the unassociated CV form (Fig. 2).

An examination of the kinetics also reveals that the change in the absorption spectrum is not associated with a free-radical mechanism. The CV reaction with $OH^\bullet$ radicals has a rate

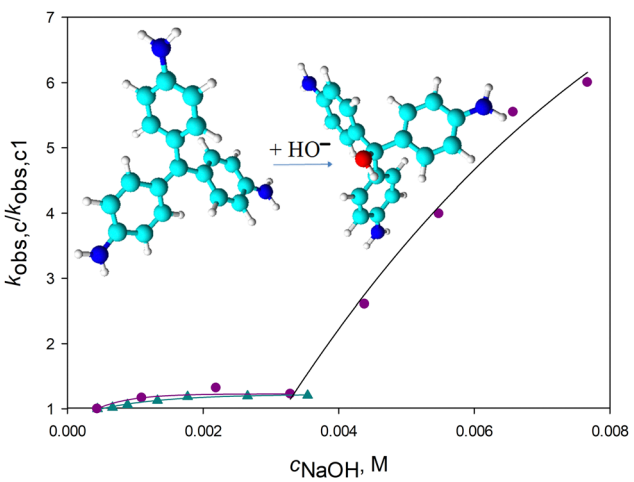

Fig. 5 Ratio of $k_{obs,c}/k_{obs,c1}$ for $CV^+ + HO^-$ (circles) and $MG^+ + HO^-$ (triangles) reactions *vs.* the NaOH concentration, where $k_{obs,c}$ is the rate constant value in alkali solution of 20 μM MS2 at 25 °C and $k_{obs,c1}$ is the rate constant value at $c_{NaOH} = 4.4 \times 10^{-4}$ M. The inset shows scheme of the reaction of CV^+ with a hydroxide ion.

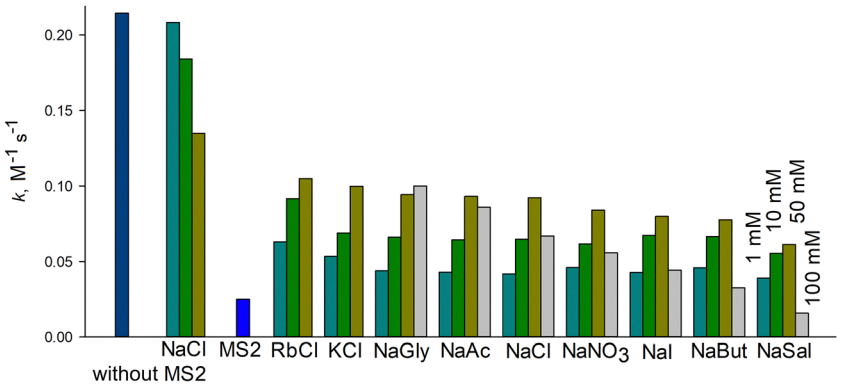

Fig. 6 Rate constant values for the $CV^+ + HO^-$ reaction in salt solutions of 4×10^{15} PFU per mL MS2 at 25 °C and c_{NaOH} = 1 mM, including an example without MS2 for comparison.

constant of $(8.0 \pm 0.6) \times 10^9$ M^{-1} s^{-1} and initially generates an adduct which subsequently dissociates to form the radical dye dication with λ_{max} = 380 nm.[68] The CV radical formed by visible light irradiation in poly(vinyl alcohol) film has λ_{max} = 408 nm.[69]

The addition of inert salt altered the reaction rate at c_{NaOH} = 1 mM; namely, in general (see Fig. 6 and Fig. S19), the trend was k_{obs}(MS2) < k_{obs}(MS2 + salt) < k_{obs}(salt), where k_{obs}(MS2) is the observed reaction rate in MS2 solution; k_{obs}(MS2 + salt) is the observed reaction rate in MS2 solution with the addition of 1 mM of salt; and k_{obs}(salt) is the observed reaction rate in MS2-free solution with the addition of 1 mM of salt. A detailed analysis of the empirical data allows us to define the following features. The accelerating effect of 1 mM of salt increases in terms of the cation for a given anion in the order $Na^+ < K^+ < Rb^+$. At 100 mmol of sodium salt, the accelerating effect decreases in terms of the anion as follows: $Gly^- < Ac^- < Cl^- < NO_3^- < I^- < But^- < Sal^-$. These salt effects reinforce and complement the following two major factors relating to electrolyte action. (i) The cation influence is due to the screening of the negative surface charge. MD simulations by Farafonov *et al.*[9] revealed that a pronounced layer of sodium ions forms a diffuse layer on the outer surface of the capsid; thus, the surface can be considered as a continuum characterized by the zeta potential. The repulsion of HO^- decreases too, but still its concentration on the negative patch is less than in the bulk phase; it is displaced by salt anions (see the influence of anions). After all, CV^+ metachromasia did not enhance in these systems, as was observed with a slight increase in alkali concentration in Fig. 2. Continuing the trend from the preceding section, the above order of cations demonstrates their electrostatic attraction to the outer surface and corresponds to an increase in the Gibbs energy of hydration for monocations.[64] (ii) The anion influence has another kinetic effect, namely a decrease in HO^- concentration associated with ion exchange between a salt anion in the bulk phase and a hydroxide ion on the phage surface: $HO_s^- + X_w^- \rightleftarrows HO_w^- + X_s^-$.[70] Consequently, the above series of anions demonstrates the affinity of small ions for the surface due to their weak hydration in the bulk phase and electrostatic interactions.[64] The effects of 10 and 50 mM additions are the result of the effects of both cations and anions. The more pronounced cation influence at 1 mM emphasises the weak affinity of anions for the domain.

4. Conclusions

Advancing the investigation of MS2 properties in terms of physicochemical characteristics involves describing its interactions with ions in aqueous systems. Studying the chemical kinetics, along with solvatochromism and metachromasia, proved to be a powerful and effective tool for investigating interparticle interactions involving biological objects. Special attention should be paid to the kinetic data showing that the MS2 phage decelerates the alkaline fading of cationic dyes, which can, for example, prevent photosynthesis. Comparing MG and CV, the latter dye proved to be a more powerful tool owing to the association that is hypothesized to occur *via* supramolecular salt bridges between negative groups of phages and the cationic groups of CV^+, which is detectable in a simple protocol by spectrophotometry. The absorption band broadening visually manifests as a less intense colour of the CV solution, and this can be confused with fading.

The monotonic changes and turning points of solvatochromism, metachromasia, and rate constants served as responses. Changing the alkalinity of the system led to responses corresponding to the pH ranges for the deprotonation of the lysine side chain, the guanidinium group, and the phenolic OH of MS2 phages. Changing the salt provided responses that agreed with the hydration energy series of cations and anions. Effects from varying the solution temperature were related to the MS2 disruption point. The experimental data agree with the results from other methods, implying that the implementation of such simple approaches is feasible for studying other systems.

Conflicts of interest

There are no conflicts to declare.

Data availability

Data relating to this article are available at Zenodo at https://doi.org/10.5281/zenodo.18760674.

Supplementary information (SI): absorption spectra of CV^+ and MG^+ in solutions of 4×10^{15} PFU per mL MS2 with salts

or/and alkali; the influence of temperature on absorption spectra of CV in solutions of 4×10^{15} PFU per mL MS2 at 0.01 M NaCl; and the rate constant values of $MG^+ + HO^-$ reaction in salt solutions (PDF). See DOI: https://doi.org/10.1039/d6cp00680a.

Acknowledgements

This project has received funding through the SAFE – ''Supporting At-Risk Researchers with Fellowships in Europe'' project, which is funded by the European Union under the Grant Agreement ref. 101148456. The views and opinions expressed are, however, those of the author(s) only and do not necessarily reflect those of the European Union or the European Research Executive Agency (REA). Neither the European Union nor the European Research Executive Agency (REA) can be held responsible for them. The authors are grateful to Zita Balklava and James Harrison, College of Health and Life Sciences, Aston University, Birmingham, U.K., for helping with MS2 stock solution preparation and purification.

References

1 P. A. de Jonge, F. L. Nobrega, S. J. J. Brouns and B. E. Dutilh, Molecular and Evolutionary Determinants of Bacteriophage Host Range, *Trends Microbiol.*, 2019, **27**(1), 51–63, DOI: 10.1016/j.tim.2018.08.006.

2 F. L. Nobrega, M. Vlot, P. A. de Jonge, L. L. Dreesens, H. J. E. Beaumont, R. Lavigne, B. E. Dutilh and S. J. J. Brouns, Targeting mechanisms of tailed bacteriophages, *Nat. Rev. Microbiol.*, 2018, **16**(12), 760–773, DOI: 10.1038/s41579-018-0070-8.

3 A. G. Cobián Güemes, M. Youle, V. A. Cantú, B. Felts, J. Nulton and F. Rohwer, Viruses as Winners in the Game of Life, *Annu. Rev. Virol.*, 2016, **3**, 197–214, DOI: 10.1146/annurev-virology-100114-054952.

4 B. Koskella, New approaches to characterizing bacteria–phage interactions in microbial communities and microbiomes, *Environ. Microbiol. Rep.*, 2019, **11**(1), 15–16, DOI: 10.1111/1758-2229.12706.

5 J. R. Whitaker, R. E. Feeney and M. M. Sternberg, Chemical and physical modification of proteins by the hydroxide ion, *Crit. Rev. Food Sci. Nutr.*, 1983, **19**(3), 173–212, DOI: 10.1080/10408398309527375.

6 Y. Feng, S. Ong, J. Hu, X. Tan and W. Ng, Effects of pH and temperature on the survival of coliphages MS2 and Qβ, *J. Ind. Microbiol. Biotechnol.*, 2003, **30**(9), 549–552.

7 K. Toropova, G. Basnak, R. Twarock, P. G. Stockley and N. A. Ranson, The three-dimensional structure of genomic RNA in bacteriophage MS2: implications for assembly, *J. Mol. Biol.*, 2008, **375**(3), 824–836, DOI: 10.1016/j.jmb.2007.08.067.

8 V. S. Farafonov, M. Stich and D. A. Nerukh, Complete Virion Simulated: All-Atom Model of an MS2 Bacteriophage with Native Genome, *J. Chem. Theory Comput.*, 2023, **19**(21), 7924–7933.

9 V. S. Farafonov and D. Nerukh, MS2 bacteriophage capsid studied using all-atom molecular dynamics, *Interface Focus*, 2019, **9**(3), 20180081.

10 K. Valegård, L. Liljas, K. Fridborg and T. Unge, The three-dimensional structure of the bacterial virus MS2, *Nature*, 1990, **345**(6270), 36–41, DOI: 10.1038/345036a0.

11 N. Vodolazkaya, M. Nikolskaya, A. Laguta, V. Farafonov, Z. Balklava, M. Stich, N. Mchedlov-Petrossyan and D. Nerukh, Estimation of Nanoparticle's Surface Electrostatic Potential in Solution Using Acid–Base Molecular Probes. III. Experimental Hydrophobicity/Hydrophilicity and Charge Distribution of MS2 Virus Surface, *J. Phys. Chem. B*, 2022, **126**(41), 8166–8176, DOI: 10.1021/acs.jpcb.2c04491.

12 A. Brié, I. Bertrand, M. Meo, N. Boudaud and C. Gantzer, The effect of heat on the physicochemical properties of bacteriophage MS2, *Food Environ. Virol.*, 2016, **8**, 251–261.

13 P. Attard, Recent advances in the electric double layer in colloid science, *Curr. Opin. Colloid Interface Sci.*, 2001, **6**(4), 366–371.

14 J. N. Israelachvili and R. M. Pashley, Measurement of the hydrophobic interaction between two hydrophobic surfaces in aqueous electrolyte solutions, *J. Colloid Interface Sci.*, 1984, **98**(2), 500–514, DOI: 10.1016/0021-9797(84)90177-2.

15 A. Kryshtal, N. Mchedlov-Petrossyan, A. Laguta, N. Kriklya, A. Kruk and E. Osawa, Primary detonation nanodiamond particles: Their core-shell structure and the behavior in organo-hydrosols, *Colloids Surf., A*, 2021, **614**, 126079.

16 N. Vodolazkaya, A. Laguta, V. Farafonov, M. Nikolskaya, Z. Balklava, R. Khayat, M. Stich, N. Mchedlov-Petrossyan and D. Nerukh, Influence of various colloidal surfactants on the stability of MS2 bacteriophage suspension. The charge distribution on the PCV2 virus surface, *J. Mol. Liq.*, 2023, **387**, 122644, DOI: 10.1016/j.molliq.2023.122644.

17 M. Raja and E. Vales, Effects of sodium chloride on membrane fusion and on the formation of aggregates of potassium channel KcsA in Escherichia coli membrane, *Biophys. Chem.*, 2009, **142**(1–3), 46–54.

18 E. K. Punch, S. Hover, H. T. Blest, J. Fuller, R. Hewson, J. Fontana, J. Mankouri and J. N. Barr, Potassium is a trigger for conformational change in the fusion spike of an enveloped RNA virus, *J. Biol. Chem.*, 2018, **293**(26), 9937–9944.

19 A. N. Laguta, S. V. Eltsov and N. O. Mchedlov-Petrossyan, Kinetics of alkaline fading of methyl violet in micellar solutions of surfactants: Comparing Piszkiewicz's, Berezin's, and pseudophase ion-exchange models, *Int. J. Chem. Kinet.*, 2019, **51**(2), 83–94, DOI: 10.1002/kin.21231.

20 A. Marini, A. Muñoz-Losa, A. Biancardi and B. Mennucci, What is solvatochromism?, *J. Phys. Chem. B*, 2010, **114**(51), 17128–17135.

21 A. N. Laguta, S. V. Eltsov and N. O. Mchedlov-Petrossyan, Micellar rate effects on the kinetics of nitrophenol violet anion reaction with HO–ion: Comparing Piszkiewicz's, Berezin's, and Pseudophase Ion-Exchange models, *J. Mol. Liq.*, 2019, **277**, 70–77, DOI: 10.1016/j.molliq.2018.12.012.

22 C. Hansch; A. Leo and D. Hoekman, *Exploring QSAR: hydrophobic, electronic, and steric constants*, American Chemical Society, Washington, DC, 1995.
23 A. Y. Wells and N. P. Sherwood, Selective action of crystal violet and of brilliant green on bactériophages, *J. Infect. Dis.*, 1933, 209–213.
24 D. Graham and F. Nelson, Inhibition of lactic streptococcus bacteriophage by crystal violet and other agents, *J. Gen. Physiol.*, 1953, **37**(1), 121–138.
25 E. W. Schultz, Inactivation of Staphyloccus Bacteriophage by Methylene Blue, *Proc. Soc. Exp. Biol. Med.*, 1928, **26**(2), 100–101, DOI: 10.3181/00379727-26-4158.
26 J. H. Shin, S. B. Jeong, I. H. Kim, S. Y. Lee, G. B. Hwang, I. Park, K. J. Heo and J. H. Jung, Performance comparison of photodynamic antimicrobial chemotherapy with visible-light-activated organic dyes: Rose bengal, crystal violet, methylene blue, and toluidine blue O, *Environ. Res.*, 2023, **238**, 117159, DOI: 10.1016/j.envres.2023.117159.
27 G. N. Lewis and M. Calvin, The Color of Organic Substances, *Chem. Rev.*, 1939, **25**(2), 273–328.
28 D. F. Duxbury, The photochemistry and photophysics of triphenylmethane dyes in solid and liquid media, *Chem. Rev.*, 1993, **93**(1), 381–433.
29 G. W. Gray, Steric Effects in Conjugated Systems, *Nature*, 1958, **182**(4635), 568–570, DOI: 10.1038/182568a0.
30 A. Schäfer, S. Giannini, D. Strelnikov, T. Mohr, F. Santoro, J. Cerezo and M. M. Kappes, Influence of symmetry breaking on the absorption spectrum of crystal violet: from isolated cations at 5 K to room temperature solutions, *Phys. Chem. Chem. Phys.*, 2024, **26**(45), 28514–28524.
31 K. Rybakova and V. Kostjukov, TD-DFT analysis of photo-induced distortions and vibronic absorption of the malachite green dye in aqueous solution, *Theor. Chem. Acc.*, 2025, **145**(1), 6, DOI: 10.1007/s00214-025-03249-7.
32 C. Dharmayanti, T. Gillam, M. Klingler-Hoffmann, H. Albrecht and A. Blencowe, Strategies for the Development of pH-Responsive Synthetic Polypeptides and Polymer-Peptide Hybrids: Recent Advancements, *Polymers*, 2021, **13**, 624, DOI: 10.3390/polym13040624.
33 C. A. Fitch, G. Platzer, M. Okon, B. Garcia-Moreno E, and L. P. McIntosh, Arginine: Its pKa value revisited, *Protein Sci.*, 2015, **24**(5), 752–761.
34 L. C. Brandão-Lima, F. C. Silva, P. V. Costa, E. A. Alves-Júnior, C. Viseras, J. A. Osajima, L. R. Bezerra, J. F. de Moura, A. G. de A. Silva and M. G. Fonseca, Clay mineral minerals as a strategy for biomolecule incorporation: Amino acids approach, *Materials*, 2021, **15**(1), 64.
35 A.-S. Yang and B. Honig, On the pH dependence of protein stability, *J. Mol. Biol.*, 1993, **231**(2), 459–474.
36 D. M. Small, D. J. Cabral, D. P. Cistola, J. S. Parks and J. A. Hamilton, The ionization behavior of fatty acids and bile acids in micelles and membranes, *Hepatology*, 1984, **4**, 77S–79S, DOI: 10.1002/hep.1840040814.
37 D. J. Cabral, J. A. Hamilton and D. M. Small, The ionization behavior of bile acids in different aqueous environments, *J. Lipid Res.*, 1987, **27**(3), 334–343, DOI: 10.1016/S0022-2275(20)38839-8.
38 M. Poša, A. Pilipović, K. Popović and D. Kumar, Thermodynamics of trimethyltetradecylammonium bromide–sodium deoxycholate binary mixed micelle formation in aqueous solution: Regular solution theory with mutual compensation of excess configurational and excess conformational entropy, *J. Mol. Liq.*, 2022, **360**, 119473, DOI: 10.1016/j.molliq.2022.119473.
39 C. Z. Ni, C. A. White, R. S. Mitchell, J. Wickersham, R. Kodandapani, D. S. Peabody and K. R. Ely, Crystal structure of the coat protein from the GA bacteriophage: model of the unassembled dimer, *Protein Sci.*, 1996, **5**(12), 2485–2493.
40 G. M. Cooper and R. E. Hausman, *The cell: a molecular approach*, Artmed Editora, 2016.
41 J. Kyte and R. F. Doolittle, A simple method for displaying the hydropathic character of a protein, *J. Mol. Biol.*, 1982, **157**(1), 105–132.
42 R. W. Sabnis, *Handbook of biological dyes and stains: synthesis and industrial applications*, John Wiley & Sons, 2010.
43 K. Bobrowski, G. Dzierzkowska, J. Grodkowski, Z. Stuglik, Z. Zagórski and W. McLaughlin, A pulse radiolysis study of the leucocyanide of malachite green dye in organic solvents, *J. Phys. Chem.*, 1985, **89**(20), 4358–4366.
44 Q. Cen, Y. He, M. Xu, J. Wang and Z. Wang, Wavelength dependent resonance Raman band intensity of broadband stimulated Raman spectroscopy of malachite green in ethanol, *J. Chem. Phys.*, 2015, **142**(11), 114201.
45 J. Korppi-Tommola and R. Yip, Solvent effects on the visible absorption spectrum of crystal violet, *Can. J. Chem.*, 1981, **59**(2), 191–194.
46 A. Laguta and S. Eltsov, Micellar effects in kinetics of interaction of malachite green and brilliant green with water, *Kharkov Univ. Bull., Chem. Ser.*, 2017, **28**(51), 96–103, DOI: 10.26565/2220-637X-2017-28-14.
47 V. S. Farafonov, A. V. Lebed and N. O. Mchedlov-Petrossyan, Solvatochromic betaine dyes of different hydrophobicity in ionic surfactant micelles: Molecular dynamics modeling of location character, *Colloids Surf., A*, 2018, **538**, 583–592, DOI: 10.1016/j.colsurfa.2017.11.046.
48 A. C. Dumetz, A. M. Chockla, E. W. Kaler and A. M. Lenhoff, Effects of pH on protein–protein interactions and implications for protein phase behavior, *Biochim. Biophys. Acta, Proteins Proteomics*, 2008, **1784**(4), 600–610.
49 G. N. Lewis, T. T. Magel and D. Lipkin, Isomers of crystal violet ion. Their absorption and re-emission of light, *J. Am. Chem. Soc.*, 1942, **64**(8), 1774–1782.
50 C. S. Oliveira, E. L. Bastos, E. L. Duarte, R. Itri and M. S. Baptista, Ion pairs of crystal violet in sodium bis (2-ethylhexyl) sulfosuccinate reverse micelles, *Langmuir*, 2006, **22**(21), 8718–8726.
51 H. B. Lueck, B. L. Rice and J. L. McHale, Aggregation of triphenylmethane dyes in aqueous solution: dimerization and trimerization of crystal violet and ethyl violet, *Spectrochim. Acta, Part A*, 1992, **48**(6), 819–828.

52 K. V. Roshchyna, S. V. Eltsov, A. N. Laguta and N. O. Mchedlov-Petrossyan, Micellar rate effects in the alkaline fading of crystal violet in the presence of various surfactants, *J. Mol. Liq.*, 2015, **201**, 77–82, DOI: 10.1016/j.molliq.2014.11.013.
53 H. E. Toma and S. Nikolaou, Self-Assembly of a Supramolecular Cyclic Polymer Containing Pyrazine Bridged Trinuclear M-Oxo-Ruthenium-Acetate Clusters, *J. Chem. Res.*, 2000, **2000**(7), 326–327.
54 L. G. Rio and A. Godoy, Influence of CTACl cationic micelles on the spectral behavior of crystal violet, *Chem. Phys.*, 2006, **327**(2–3), 361–367.
55 C. S. Oliveira, K. P. Branco, M. S. Baptista and G. L. Indig, Solvent and concentration effects on the visible spectra of tri-para-dialkylamino-substituted triarylmethane dyes in liquid solutions, *Spectrochim. Acta, Part A*, 2002, **58**(13), 2971–2982.
56 C. Capici, G. Gattuso, A. Notti, M. F. Parisi, S. Pappalardo, G. Brancatelli and S. Geremia, Selective Amine Recognition Driven by Host–Guest Proton Transfer and Salt Bridge Formation, *J. Org. Chem.*, 2012, **77**(21), 9668–9675, DOI: 10.1021/jo301730m.
57 O. Rolfsson, K. Toropova, V. Morton, S. Francese, G. Basnak, G. S. Thompson, S. W. Homans, A. E. Ashcroft, N. J. Stonehouse and N. A. Ranson, *et al.*, RNA packing specificity and folding during assembly of the bacteriophage MS2, *Comput. Math. Methods Med.*, 2008, **9**(3–4), 339–349, DOI: 10.1080/17486700802168445.
58 R. I. Koning, J. Gomez-Blanco, I. Akopjana, J. Vargas, A. Kazaks, K. Tars, J. M. Carazo and A. J. Koster, Asymmetric cryo-EM reconstruction of phage MS2 reveals genome structure in situ, *Nat. Commun.*, 2016, **7**(1), 12524, DOI: 10.1038/ncomms12524.
59 R. Koning, S. van den Worm, J. R. Plaisier, J. van Duin, J. Pieter Abrahams and H. Koerten, Visualization by Cryo-electron Microscopy of Genomic RNA that Binds to the Protein Capsid Inside Bacteriophage MS2, *J. Mol. Biol.*, 2003, **332**(2), 415–422, DOI: 10.1016/S0022-2836(03)00846-5.
60 J. L. Marco-Brown, L. Guz, M. S. Olivelli, B. Schampera, R. M. Torres Sánchez, G. Curutchet and R. Candal, New insights on crystal violet dye adsorption on montmorillonite: Kinetics and surface complexes studies, *Chem. Eng. J.*, 2018, **333**, 495–504, DOI: 10.1016/j.cej.2017.09.172.
61 K. Vus, U. Tarabara, Z. Balklava, D. Nerukh, M. Stich, A. Laguta, N. Vodolazkaya, N. O. Mchedlov-Petrossyan, V. Farafonov and N. Kriklya, Association of novel monomethine cyanine dyes with bacteriophage MS2: A fluorescence study, *J. Mol. Liq.*, 2020, **302**, 112569.
62 A. X. P. D'mello, T. V. Sylvester, V. Ramya, F. P. Britto, P. K. Shetty and S. Jasphin, Metachromasia and metachromatic dyes: a review, *Int. J. Adv. Health Sci.*, 2016, **2**(10), 12–17.
63 A. Laguta, A. Ronco-Campaña and A. D. Goddard, Styrene maleic acid lipid particles: Characterization using indicators and dyes as tools, *J. Mol. Liq.*, 2024, **405**, 125080, DOI: 10.1016/j.molliq.2024.125080.
64 Y. Marcus, Thermodynamics of solvation of ions. Part 5. Gibbs free energy of hydration at 298.15 K, *J. Chem. Soc., Faraday Trans.*, 1991, **87**(18), 2995–2999, DOI: 10.1039/FT9918702995.
65 C. M. Teschke, A. McGough and P. A. Thuman-Commike, Penton release from P22 heat-expanded capsids suggests importance of stabilizing penton-hexon interactions during capsid maturation, *Biophys. J.*, 2003, **84**(4), 2585–2592.
66 M. N. Khan, *Micellar catalysis*, CRC Press, 2006.
67 C. Reichardt and T. Welton, *Solvents and solvent effects in organic chemistry*, John Wiley & Sons, 2011.
68 R. Nakamura and M. Hida, Counter ion effect on photochemical reaction of Crystal Violet, *Sen'i Gakkaishi*, 1983, **39**(9), T360–T366.
69 A. C. Bhasikuttan, A. V. Sapre and L. V. Shastri, Oxidation of crystal violet and malachite green in aqueous solutions — a kinetic spectrophotometric study, *J. Photochem. Photobiol., A*, 1995, **90**(2), 177–182, DOI: 10.1016/1010-6030(95)04094-V.
70 C. A. Bunton, F. Nome, F. H. Quina and L. S. Romsted, Ion binding and reactivity at charged aqueous interfaces, *Acc. Chem. Res.*, 1991, **24**(12), 357–364, DOI: 10.1021/ar00012a001.

